

A step in the direction of resolving the paradox of Perdew-Zunger self-interaction correction

Rajendra R. Zope,^{1, a)} Yoh Yamamoto,¹ Carlos Diaz,¹ Tunna Baruah,¹ Juan E. Peralta,² Koblar A. Jackson,² Biswajit Santra,³ and John P. Perdew³

¹⁾ *Department of Physics, University of Texas at El Paso, El Paso, Texas 79968*

²⁾ *Physics Department and Science of Advanced Materials Program, Central Michigan University, Mt. Pleasant, Michigan 48859*

³⁾ *Physics Department, Temple University, Philadelphia, Pennsylvania 19122; Chemistry Department, Temple University, Philadelphia, Pennsylvania 19122*

(Dated: March 18, 2022)

Self-interaction (SI) error, which results when exchange-correlation contributions to the total energy are approximated, limits the reliability of many density functional approximations. The Perdew-Zunger SI correction (PZSIC), when applied in conjunction with the local spin density approximation (LSDA), improves the description of many properties, but overall, this improvement is limited. Here we propose a modification to PZSIC that uses an iso-orbital indicator to identify regions where local SI corrections should be applied. Using this local-scaling SIC (LSIC) approach with LSDA, we analyze predictions for a wide range of properties including, for atoms, total energies, ionization potentials, and electron affinities, and for molecules, atomization energies, dissociation energy curves, reaction energies, and reaction barrier heights. LSIC preserves the results of PZSIC-LSDA for properties where it is successful and provides dramatic improvements for many of the other properties studied. Atomization energies calculated using LSIC are better than those of the Perdew, Burke, and Ernzerhof (PBE) generalized gradient approximation (GGA) and close to those obtained with the Strongly Constrained and Appropriately Normed (SCAN) meta-GGA. LSIC also restores the uniform gas limit for the exchange energy that is lost in PZSIC-LSDA. Further performance improvements may be obtained by an appropriate combination or modification of the local scaling factor and the particular density functional approximation.

I. INTRODUCTION

The Kohn-Sham (KS) formulation of density functional theory (DFT) has become the most popular approach for studying the electronic, structural and other properties of molecular and condensed systems¹. KS-DFT is a formally exact theory^{1,2} to obtain the ground-state energy and electron density, but its practical realization requires an approximation to the exchange-correlation density functional. The enormous popularity of DFT is due to the combined appeal of sufficiently accurate density functional approximations (DFAs), favorable scaling with respect to the number of atoms, and numerically accurate and efficient implementations that have resulted in numerous easy-to-use codes. The local spin density approximation (LSDA)^{1,3,4}, based on the uniform electron gas model, was an early and simple DFA. The success of LSDA in describing the electronic properties of solids made DFT popular in the physics community. Careful analysis attributed this success to the spherical exchange-hole of LSDA being a good approximation to the spherical average of the exact exchange-hole and to the satisfaction of the exchange correlation hole sum rule^{3,5,6}. Subsequent improvements beyond the LSDA were obtained^{7–16} by including information about the local electron density gradient in generalized gradient

approximations (GGAs), and also the Laplacian and kinetic energy density, in meta-GGAs. The non-empirical functionals among these are designed to satisfy various constraints and norms of the exact functional, including the uniform electron gas limit¹⁷.

Extensive work has shown that local and semi-local DFAs work well when the exact exchange-correlation hole density is localized around the electron, as is usually the case near equilibrium configurations in molecules and solids. But these functionals can fail dramatically in stretched-bond situations such as in the transition states of chemical reactions and molecular dissociation¹⁷, causing the underestimation of barrier heights in chemical reactions and the incorrect dissociation of radical and heteroatomic molecules. This failure can be traced to electron self-interaction errors (SIE) caused by the incomplete cancellation of the self-Coulomb energy with the approximate self-exchange-correlation energy for one electron densities. This was recognized long ago and attempts to remove SIE were pursued^{18–22}. One widely-used approach to mitigating the effect of SIE, introduced by Becke, is by combining Hartree-Fock exchange with semi-local functionals²³. As the Hartree-Fock approximation is self-interaction free and introduces errors that are often of opposite sign to those of semi-local functionals²⁴, this approach can overcome a number of deficiencies of semi-local DFAs. The formal justification for such mixing can be obtained by an adiabatic connection^{5,6,25} between the real interacting system and the non-interacting Kohn-Sham system. Global

^{a)} Electronic mail: rzope@utep.edu

hybrids²³, local hybrids²⁶ and range-separated hybrids²⁷, are all approximations that add Hartree-Fock exchange using various criteria. A majority of these functionals, however, still suffer from non-zero SIE.

A systematic procedure for eliminating one-electron self-interaction error was given by Perdew and Zunger (PZ) in 1981²⁸. In the PZ self-interaction correction (PZSIC) approach, the SIE of a DFA is removed from the total energy in an orbital-by-orbital fashion by redefining the energy as

$$E^{PZSIC-DFA} = E^{DFA}[\rho_{\uparrow}, \rho_{\downarrow}] - \sum_i \{U[\rho_{i\sigma}] + E_{XC}^{DFA}[\rho_{i\sigma}, 0]\} \quad (1)$$

Here, $U[\rho_{i\sigma}]$ is the exact self-Coulomb energy and $E_{XC}^{DFA}[\rho_{i\sigma}, 0]$ is the approximate self-exchange and correlation energy. PZSIC-DFA is exact for any one-electron density and gives no correction to the exact functional.

One of the features of PZSIC is that $E^{PZSIC-DFA}$ is not invariant to the choice of orbitals used to represent the total electron density. Different orbitals that give the same total density yield different total energies so that finding the minimum energy formally requires searching over all sets of orbitals that span the correct density. It can be shown that the variational minimum energy corresponds to $\rho_{i\sigma} = |\phi_{i\sigma}|^2$ for orbitals $\phi_{i\sigma}$ that satisfy the set of conditions known as the Pederson or localization equations^{29,30},

$$\langle \phi_{i\sigma} | V_{i\sigma}^{SIC} - V_{j\sigma}^{SIC} | \phi_{j\sigma} \rangle = 0. \quad (2)$$

In traditional PZSIC, a unitary transformation of the KS orbitals is performed to construct the local orbitals. Optimizing the local orbitals to satisfy Eq. (2) requires tuning the $O(N^2)$ elements of the transformation matrix, which is computationally expensive.

PZSIC provided a way to go beyond the LSDA, but the computational difficulties mentioned above deterred practitioners from following this path³¹ and only a relatively few implementations of PZSIC have been reported³²⁻⁷⁰. A review³¹ by Pederson and Perdew nicely summarizes this and related work. A handful of studies involved PZSIC combined with semi-local approximations^{43-45,60,71,72}. These found that while PZSIC improves properties like the dissociation pathway of heteroatomic molecules, it worsens the good description of semi-local functionals for near-equilibrium properties such as atomization energies, due to overcorrection^{44,73}. This has come to be known as the paradox of SIC⁷⁴. A few approaches have been proposed to rectify this behavior based on scaling down the SIC contribution to the energy (second terms in the right hand side of Eq. (1)). Ref. [11] proposed to use the ratio between the von Weizsäcker and the total kinetic energy densities to identify one- and two-electron regions for meta-GGAs, and Tsuneda *et al.*⁴⁸ first proposed to use this ratio to identify one-electron regions where SIC is expected to be important. Ref. [48] replaced the DFA

energy density in these regions with an expression based on the exchange energy of hydrogenic orbitals. Later, Vydrov *et al.*⁴⁵ used a selective orbital-by-orbital scaling down of the SIC contribution to the energy, and more recently, Jónsson *et al.*⁷⁵ proposed to globally reduce the SIC energy by 50%. The Jónsson group also pioneered⁷⁶ the use of complex orbitals in PZSIC, which work well with PZSIC-PBE. The scaling approaches, which are discussed in more detail below, achieve success for selected properties, but, in general, they destroy the desirable $-1/r$ asymptotic form of the potential seen by an electron in a localized system such as a neutral atom in a PZSIC calculation⁴⁵. This unphysical behavior has important consequences for properties like charge transfer.

Considerable effort has been spent trying to understanding the origin of the PZSIC paradox. A recent study found that PZSIC raises the total energy as the nodality of the valence local orbitals increases from atoms to molecules to transition states⁷⁷. More recently, it was shown that, unlike the non-empirical semi-local functionals, PZSIC violates the uniform electron gas norm for the exchange and correlation energies⁷⁸. The implication of this is that adding PZSIC breaks the correct behavior of these functionals for slowly-varying densities.

In this work, we propose an approach that adjusts the PZSIC correction locally, that is, at each point in space, by adjusting the magnitude of the correction using an iso-orbital indicator. We call this approach local-scaling SIC (LSIC). It is implemented in the FLOSIC code^{79,80} and applied perturbatively to self-consistent PZSIC solutions obtained using the Fermi-Löwdin orbital SIC (FLO-SIC) method^{81,82}. As discussed further below, the method applies SIC at full strength for a density with a single-orbital character and turns it off for a uniform density. We assessed the predictions of this approach for a number of properties including, for atoms: total energies, ionization potentials, and electron affinities, and for molecules: atomization energies, reaction energies and dissociation energy curves, and reaction barrier heights. We find significant improvement for properties that PZSIC typically worsens, while retaining the successful predictions of PZSIC in situations where removing SIE is critical. The proposed LSIC method, unlike semi-local functionals and most earlier PZSIC implementations, provides a good description of both near-equilibrium properties and properties associated with stretched-bond situations. LSIC thus appears to resolve the paradox of PZSIC and opens the door to designing universally accurate DFAs.

II. THEORY AND COMPUTATIONAL DETAILS

The application of PZSIC worsens the quality of equilibrium properties when used with semilocal functionals^{43-45,72,76,83,84}. Attempts have been made to restore the accuracy of semi-local functionals used in combination with PZSIC by reducing the size of the corrections. For example, Jónsson and coworkers used a

scaled-down version of PZSIC in which the SIC correction is reduced by 50%⁷⁵. Such a diminished correction, when applied with the PBE functional, resulted in overall improvement of atomization energies but significant absolute errors still remained. Instead of using a fixed constant scaling factor, Vydrov and coworkers⁴⁵ had earlier proposed setting a scaling factor for each local orbital i in the following way:

$$X_{i\sigma}^k = \int \left(\frac{\tau_{i\sigma}^W}{\tau_{i\sigma}} \right)^k \rho_{i\sigma}(\vec{r}) d\vec{r}. \quad (3)$$

Here, $\tau_{i\sigma}^W(\vec{r})$ is the von Weizsäcker kinetic energy density and $\tau_{i\sigma}(\vec{r})$ is the Kohn-Sham kinetic energy density. This scaling factor is subsequently used to attenuate the Coulomb and exchange-correlation parts of the SIC as follows:

$$E^{\text{scaled-SIC}} = - \sum_{i\sigma}^{\text{occ}} X_{i\sigma}^k (U[\rho_{i\sigma}] + E_{XC}^{DFA}[\rho_{i\sigma}, 0]). \quad (4)$$

We shall refer to this approach as exterior orbital scaling. Like PZSIC, and unlike the 50% global scaling, this approach is exact for all one-electron densities and, with $k \geq 1$, for all uniform densities.

Vydrov *et al.* noted that while increasing k above zero satisfies some additional exact constraints, the correct $-1/r$ asymptotic behavior of the one electron potential is lost if $k > 0$. Vydrov and Scuseria also proposed a simpler method⁴⁷ of moderating SIC with a scaling factor given as

$$W_{i\sigma}^m = \int \left(\frac{\rho_{i\sigma}}{\rho_{\sigma}} \right)^m \rho_{i\sigma} d\vec{r} = \int \frac{\rho_{i\sigma}^{m+1}}{\rho_{\sigma}^m} d\vec{r}. \quad (5)$$

This factor depends on the ratio of overlaps of orbital density $\rho_{i\sigma}$ and the total density ρ_{σ} for a given spin σ . The authors noted that the SIC-PBE with $m = 1$ performs consistently well for the benchmark tests, but a larger value of m , such as $m = 4$, is needed for SIC-LSDA.

PZSIC improves results where semi-local functionals fail drastically on account of SIE^{45,77,85}, but it over-corrects and worsens the description of near-equilibrium properties such as molecular atomization energies. Based on this observation, we propose a modification of PZSIC in such a way that the self-interaction correction is enforced only where it is necessary. This can be done *locally*, or point-wise in space, that is, it can be applied only in the regions where self-interaction is expected to be strong. Tsuneda and coworkers⁴⁸ defined these to be regions where the density has one-electron character and they used the ratio $z_{\sigma}(\vec{r}) = \tau_{\sigma}^W(\vec{r})/\tau_{\sigma}(\vec{r})$ to identify these regions. Here the non-interacting (Kohn-Sham) kinetic energy density τ_{σ} for a spin σ is given as,

$$\tau_{\sigma}(\vec{r}) = \frac{1}{2} \sum_i |\vec{\nabla} \psi_{i\sigma}(\vec{r})|^2, \quad (6)$$

and τ_{σ}^W is given as

$$\tau_{\sigma}^W(\vec{r}) = \frac{|\vec{\nabla} \rho_{\sigma}(\vec{r})|^2}{8\rho_{\sigma}(\vec{r})}. \quad (7)$$

Since τ_{σ}^W is the single orbital limit of τ_{σ} and vanishes for a uniform density, $z_{\sigma}(\vec{r})$ varies between zero and one, with zero corresponding to uniform densities and one to one-electron densities. In their regional SIC scheme, Tsuneda and coworkers⁴⁸ used this ratio to replace the conventional DFT expression for the exchange and correlation potential in regions where z is close to one by a simple model expression intended to mimic the exchange potential of a single hydrogenic orbital. They used their scheme to study reaction barriers, where they found significant improvement over conventional DFT calculations. Following Tsuneda *et al.*, we propose the following modification to the PZSIC energy expression:

$$E_{XC}^{LSIC-DFA} = E_{XC}^{DFA}[\rho_{\uparrow}, \rho_{\downarrow}] - \sum_{i,\sigma}^{\text{occ}} \{ U^{LSIC}[\rho_{i,\sigma}] + E_{XC}^{LSIC}[\rho_{i,\sigma}, 0] \} \quad (8)$$

where

$$U^{LSIC}[\rho_{i,\sigma}] = \frac{1}{2} \int d\vec{r} \{ z_{\sigma}(\vec{r}) \}^k \rho_{i,\sigma}(\vec{r}) \int d\vec{r}' \frac{\rho_{i,\sigma}(\vec{r}')}{|\vec{r} - \vec{r}'|} \quad (9)$$

and

$$E_{XC}^{LSIC}[\rho_{i,\sigma}, 0] = \int d\vec{r} \{ z_{\sigma}(\vec{r}) \}^k \rho_{i,\sigma}(\vec{r}) \epsilon_{XC}^{DFA}([\rho_{i,\sigma}, 0], \vec{r}). \quad (10)$$

The LSIC-DFA of Eq. [8] recovers the PZSIC (Eq. [1]) for $k = 0$. The $k \rightarrow \infty$ limit, on the other hand, zeroes out the SIC and reduces thereby to a standard DFA, except in fully one-electron regions. In the present work we use $k = 1$. This is the simplest choice of scaling factor based on z_{σ} . It smoothly interpolates between uniform density regions and one-electron regions. In the rest of this section we provide the computational details.

We implemented the LSIC approach in the FLOSIC code which is based on the UTEP-NRLMOL^{79,80} software package. UTEP-NRLMOL is a modern version of the Gaussian-orbital-based NRLMOL code⁸⁶⁻⁸⁸. We use the NRLMOL default basis sets⁸⁹ that are of approximately quadruple zeta quality⁹⁰. For a better description of atomic anions, we added long range s, p, and d single Gaussian orbitals to the default NRLMOL basis set. The exponents for the additional functions were obtained from the relation $\beta(N+1) = \frac{\beta(N)}{\beta(N-1)}\beta(N)$ where $\beta(N)$ is the exponent of N -th Gaussian in the basis for a given atom. NRLMOL's variational integration mesh⁸⁷ adapts to the range of basis functions so that integrals are computed to a specified accuracy.

We use the Fermi-Löwdin Orbital Self-Interaction Correction (FLO-SIC) approach proposed by Pederson *et al.*^{81,82} to implement the PZSIC and LSIC methods. In FLO-SIC, the local orbitals used to evaluate the PZSIC

total energy are based on Fermi orbitals constructed from the density with parameters known as Fermi orbital descriptors (FODs), M positions in 3-dimensional space for M occupied orbitals. Using these FODs, one can write the Fermi orbitals as

$$F_{i\sigma}(\vec{r}) = \sum_j^M \frac{\psi_{j\sigma}^*(\vec{a}_{i\sigma})\psi_{j\sigma}(\vec{r})}{\sqrt{\rho_\sigma(\vec{a}_{i\sigma})}}, \quad (11)$$

where $\vec{a}_{i\sigma}$ is the FOD position for orbital i of spin σ , ρ_σ is the electron spin density, and $\psi_{j\sigma}$ is one of the M occupied orbitals. Since Fermi orbitals are generally not orthogonal, Löwdin orthogonalization is performed to transform the F_i into the orthonormal local orbital $\phi_{i,\sigma}$. The FLO-SIC approach is unitarily invariant because any set of orbitals spanning the occupied orbital space can be used in Eq. [11] to generate the Fermi orbitals. To minimize the PZSIC energy, the $3N$ FOD positions must be optimized. This is done using gradients of the energy with respect to the FOD positions⁹¹ in a manner analogous to a molecular geometry optimization. This is a computationally simpler process than determining the $O(N^2)$ parameters required to define the local orbital transformation in traditional PZSIC. We follow the self-consistency procedure of Ref. [92]. Iteration averaging was performed for the DFA potentials, using either Broyden mixing or simple mixing scheme to accelerate convergence. A self-consistency convergence tolerance of 10^{-6} Ha in the total energy was used for all calculations. For PZSIC calculations using FLOSIC, an FOD force tolerance of 10^{-3} Ha/Bohr was used to ensure optimized FOD positions. LSIC-LSDA total energies (Eq. (8)) were computed using the corresponding self-consistent PZSIC-LSDA density and optimized local orbitals. Both LSIC and FLO-SIC calculations have similar computational costs. The only additional quantity needed for LSIC is the scaling factor, which requires the evaluation of the kinetic energy densities whose computational cost is negligible. The FLO-SIC methodology has been recently employed to study atomic energies⁹³, atomic polarizabilities⁸³, and magnetic exchange couplings⁹⁴.

III. RESULTS

A. Atoms

1. Total Energy

We compared the total energy E of atoms for atomic numbers $Z = 1 - 18$ computed using different methods against the accurate non-relativistic energies (E_{accu}) reported by Chakravorty *et al.*⁹⁵. The total energy differences $E - E_{\text{accu}}$ are shown in Fig. 1 for LSDA, PZSIC-LSDA, and LSIC-LSDA. In general, LSDA overestimates the total energies and applying SIC shifts the energies in the proper direction. But the corrections are too large and PZSIC-LSDA predicts atomic energies that are too

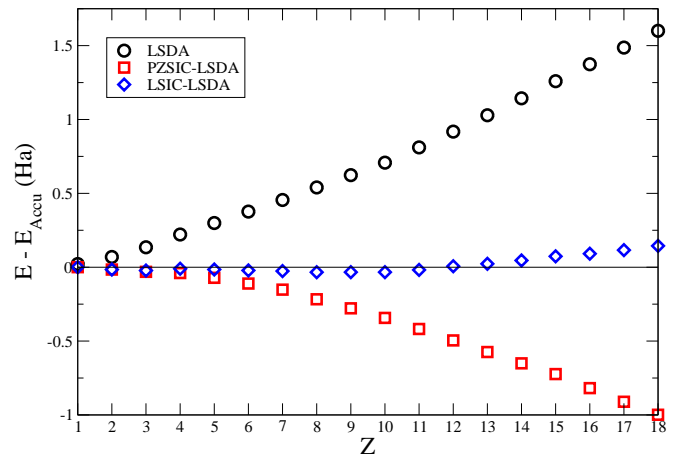


Figure 1. LSDA, PZSIC-LSDA, and the LSIC-LSDA total energies of atoms $Z = 1 - 18$, relative to reference energies (E_{accu}) from Ref. [95].

Table I. MAE of atom total energies $Z=1-18$ (Ha)

Method	MAE
LSDA ^a	0.726
PBE ^a	0.083
SCAN ^a	0.019
PZSIC-LSDA ^a	0.381
PZSIC-PBE ^a	0.159
PZSIC-SCAN ^a	0.147
LSIC-LSDA	0.041

^a Reference⁷².

low. The LSIC-LSDA total energies, by contrast, are very close to the reference energies. LSIC reduces the mean absolute errors (MAE) in the energies by an order of magnitude compared to PZSIC-LSDA. The MAE are 0.726, 0.381, and 0.041 Ha for LSDA, PZSIC-LSDA, and LSIC-LSDA, respectively. Results for atomic total energies for a variety of methods are summarized in Table I. The LSIC-LSDA results are better than PBE, but slightly worse than SCAN.

2. Ionization potential

Since the ionization potential is the energy required to remove an electron from the outermost orbital, this quantity is sensitive to the asymptotic behavior of the potential and can be expected to be affected by SIC, especially for large systems. We calculated the ionization potential (IP) for the atoms He-Kr using the Δ SCF approach

$$E_{IP} = E_{\text{cation}} - E_{\text{neutral}}. \quad (12)$$

Fig. 2 shows a comparison of calculated IPs against experimental values for LSDA, PZSIC-LSDA, and LSIC-LSDA. The MAEs are presented in Table II, along with

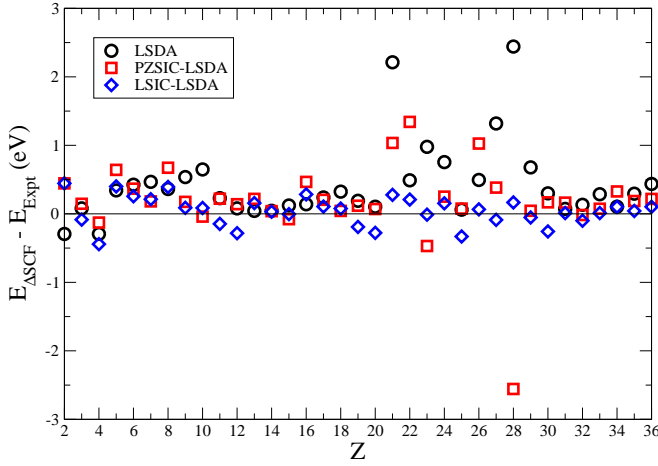


Figure 2. Ionization potential of atoms $Z = 2 - 36$. LSDA, PZSIC-LSDA, and the LSIC-LSDA are shown.

Table II. MAE of Δ SCF ionization potentials (eV)

Method	Z=2–18 (17 IPs) MAE	Z=2–36 (35 IPs) MAE
LSDA	0.275	0.458
PBE	0.159	0.253
SCAN	0.175	0.273
PZSIC-LSDA	0.248	0.364
PZSIC-PBE	0.405	0.464
PZSIC-SCAN	0.274	0.259
LSIC-LSDA	0.206	0.170

results for other methods. From LSDA to PZSIC, the IPs improve noticeably, with the MAE dropping from 0.458 to 0.364 eV. LSIC further improves the IPs, reducing the MAE down to 0.170 eV. Because the LSIC-LSDA total energies for the neutral atoms are very close to the reference energies, the accurate IP values imply that the LSIC-LSDA cation energies are also quite accurate. In Table II we show the results for the atoms from He–Ar and for all atoms in separate columns, to distinguish the performance for light versus heavy atoms. PBE and SCAN perform well for the lighter atoms, but less so for the heavier ones. LSIC-LSDA, on the other hand, performs equally well for all atoms. LSIC-LSDA performs better than both PBE and SCAN (MAE 0.253 and 0.273 eV, respectively) for the 35 IPs.

3. Electron affinity

The electron affinities (EA) of atoms from H to Br were also investigated. As in the case of the IPs, the EAs were calculated using the Δ SCF method, taking the total energy differences of the neutral atoms and their anions. We considered the twenty atoms in the first three rows (H, Li, B, C, O, F, Na, Al, Si, P, S, Cl, K, Ti, Cu, Ga, Ge, As, Se, and Br) with stable anions and for which experimental EAs are available⁹⁶. Fig. 3 shows the results

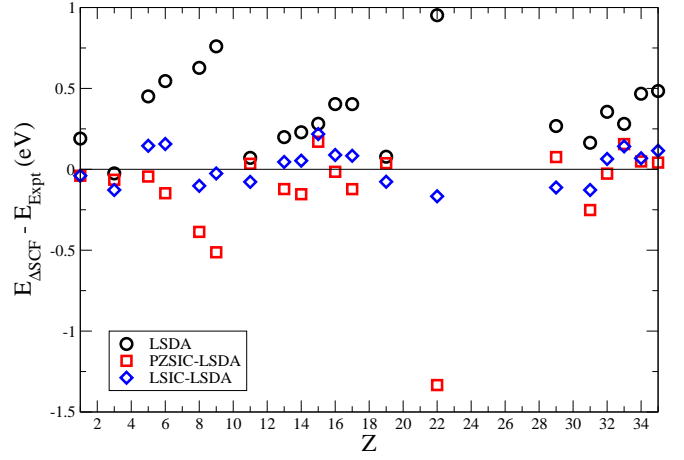


Figure 3. Electron affinity of atoms $Z = 1 - 35$. LSDA, PZSIC-LSDA, and the LSIC-LSDA are shown where experimental values are reported.

for each atom for LSDA, PZSIC-LSDA, and LSIC-LSDA. In Table III we again analyze the performance of various methods, dividing the results into two groups, the first containing the 12 EAs corresponding to first and second row atoms and the second containing all 20 EAs. The MAE relative to experiment are shown in the table. We note that although the Δ SCF approach yields positive EAs for the DFAs, the eigenvalue corresponding to the added electron becomes positive in all DFA anion calculations, indicating that the extra electron is not actually bound in the complete basis set limit. This problem is due to the incorrect asymptotic form of the potential in the DFA calculations. SIC rectifies this²⁸, leading to bound states for the HOMO in the anions. Nevertheless, we include the EAs of DFA calculations based on the Δ SCF approach in Table III for comparison purposes. We note that these results compare well with PZSIC results of Vydrov and Scuseria⁴⁵.

Overall, LSDA overestimates the values of the EAs, whereas PZSIC-LSDA tends to underestimate them, particularly for O, F, and Ti. The LSIC-LSDA method improves the EA values so that they consistently fall within ± 0.2 eV of the experimental values. The MAE of 20 EAs is reduced from 0.362 eV for LSDA, to 0.189 eV for PZSIC-LSDA, to 0.102 eV for LSIC-LSDA.

B. Atomization energy

The atomization energy (AE) of a molecule is defined as

$$AE = \sum_i^{N_{atom}} E_i - E_{mol} > 0, \quad (13)$$

where E_i is the energy of an individual atom and E_{mol} is the energy of the molecule. We computed AE s for a diverse set consisting of 37 molecules. The majority of

Table III. MAE of Δ SCF electron affinities (eV)

Method	12 EAs MAE	20 EAs MAE
LSDA ^{a,b}	0.349	0.362
PBE ^{a,b}	0.167	0.172
SCAN ^{a,b}	0.115	0.148
PZSIC-LSDA ^a	0.151	0.189
PZSIC-PBE ^a	0.534	0.531
PZSIC-SCAN ^a	0.364	0.341
LSIC-LSDA	0.097	0.102

^a Reference⁷².^b DFA results are based on total energies. The eigenvalue of the extra electron becomes positive.

the molecules were taken from the G2/97 test set⁹⁷. We also included the six systems from the AE6 test set⁹⁸. All molecular geometries were taken from Ref. [96] (B3LYP and the 6-31G(2df,p) basis) except O₂, CO, CO₂, C₂H₂, Li₂, CH₄, NH₃, and H₂O, which were obtained using PBE and the default NRLMOL basis set.

The percentage errors in calculated *AEs* relative to experiment are shown in Fig. 4 for LSDA, PZSIC-LSDA, and LSIC-LSDA. LSDA significantly overestimates the *AEs*. PZSIC-LSDA tends to improve them, but in most cases still overestimates their values. LSIC-LSDA reduces the *AEs* further, bringing them into better agreement with experiment. Mean absolute percentage errors (MAPE) for a variety of methods are compared in Table IV. The MAPE for the full set of molecules is 24.21 % for LSDA, 13.42 % for PZSIC-LSDA, and 6.94 % for LSIC-LSDA. The performance of the LSIC-LSDA falls between that of PBE (8.64 %) and SCAN (5.22 %). We also list results for the AE6 test set in Table IV, showing both the MAE and MAPE. The AE6 molecules are intended to give a good representative of atomization energy performance. Here, too, it can be seen that LSIC-LSDA has a performance that is better than PBE, though not as good as SCAN.

C. SIE Test Sets

Recently, Sharkas *et al.*⁸⁵ used the FLO-SIC methodology to study the performance of the PZSIC for a test set consisting of dissociation energies⁹⁹ (SIE4 \times 4) and reaction energies¹⁰⁰ (SIE11) that are expected to be strongly affected by self-interaction errors in DFAs. They found that PZSIC significantly decreases the errors of LSDA and PBE relative to reference calculations using the coupled-cluster with singles, doubles and perturbative triple excitations (CCSD(T)) method. We studied the same test sets using LSIC-LSDA. The SIE4 \times 4 set consists of four symmetric dimer cations at four different dimer separations *R* relative to the respective equilibrium separations *R_e*: *R/R_e* = 1, 1.25, 1.5, and 1.75. The SIE11 set consists of six cationic reactions (of which four are the dimer cations from the SIE4 \times 4 data set at their

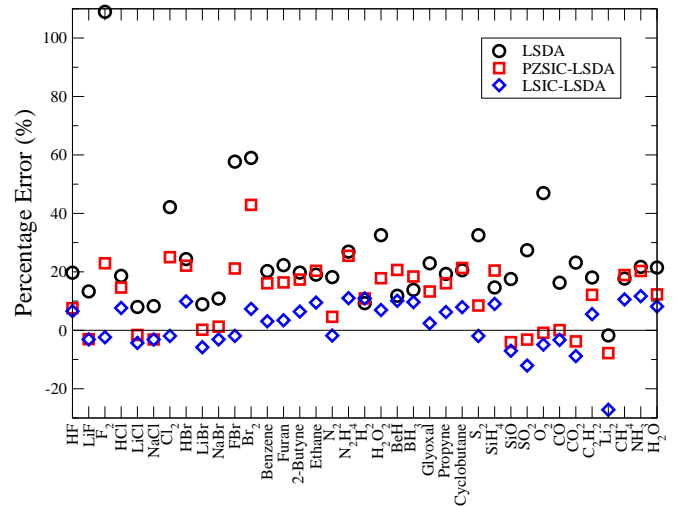


Figure 4. Percentage errors for calculated atomization energies relative to experimental values. Results for the LSDA, PZSIC-LSDA, and LSIC-LSDA methods are shown.

equilibrium geometries) and five neutral reactions. We use the atomic geometries and FOD positions found in the supplementary information of Ref. [85] as starting points for our FLO-SIC-LSDA calculations. We re-optimized the FOD positions to ensure the FOD forces were below the 10^{-3} Ha/Bohr threshold.

Results for the individual cases in the test sets are shown in Table V for LSDA, PZSIC-LSDA, and LSIC-LSDA. Results are given as signed errors (in kcal/mol) relative to accurate reference values (also shown). For the SIE4 \times 4 case, PZSIC-LSDA and LSIC-LSDA clearly improve on the results of LSDA for all separations. The PZSIC results are generally better than LSIC for *R/R_e* > 1, though the differences are small compared to the scale of the self-interaction corrections. Conversely, the LSIC results are consistently better near *R_e*. The mean average error (MAE) is slightly smaller in LSIC than in PZSIC, 2.6 versus 3.0 kcal/mol, respectively. For the SIE11 test set, the signed errors are typically somewhat smaller in LSIC than in PZSIC. In the case of the dissociation of (CH₃)₂CO⁺ there is a dramatic reduction in the signed error. This drops the MAE for the SIE11 cationic reactions from 14.83 for PZSIC to 2.31 kcal/mol for LSIC. The MAE for the SIE11 neutral reactions also shows an improvement from 9.01 to 6.31 kcal/mol.

The LSIC-LSDA results are also as good or better than PZSIC-PBE results, which have MAE of 2.3, 8.7 and 7.9 kcal/mol for SIE4 \times 4, SIE11 cationic, and SIE11 neutral, respectively.

Fig. 5 shows ground-state dissociation curves for H₂⁺ and He₂⁺. These give useful comparisons of the overall behavior of PZSIC-LSDA and LSIC-LSDA with that of LSDA and PBE both near and far from the equilibrium separations. In both cases, the DFA calculations produce qualitatively incorrect energy curves as the interatomic separation increases, featuring a slight energy

Table IV. Atomization energies: AE6 errors (MAE and MAPE) and errors for the full set (MAPE) are shown.

Method	AE6 MAE (kcal/mol)	AE6 MAPE (%)	37 molecules MAPE (%)
LSDA	74.26	15.93	24.21
PBE	13.43	3.31	8.64
SCAN	2.85	1.15	5.22
PZSIC-LSDA	57.97	9.37	13.42
PZSIC-PBE	18.83	6.82	9.67
PZSIC-SCAN	16.31	5.64	10.24
LSIC-LSDA	9.95	3.20	6.94

barrier at large separations on the way to a too-low energy for the dissociation products, two $H^{+0.5}$ or $He^{+0.5}$ fragments. Both PZSIC and LSIC calculations restore the correct qualitative shape to the dissociation curves. In the case of H_2^+ , PZSIC and LSIC give identical and exact results, because the iso-orbital indicator z_σ is exactly one everywhere for this one-electron case. For He_2^+ , LSIC and PZSIC give the same results in the dissociation limit of He and He^+ , since both of these are also one-electron systems (He has one-electron of each spin). Near the equilibrium separation, however, LSIC reduces the size of the self-interaction correction, resulting in a binding energy that is close to that of PBE.

D. Barrier heights of chemical reactions

To investigate the performance of LSIC for barrier heights in chemical reactions, we used the BH6 test set. This is a representative subset of the BH24 set¹⁰³. The reactions included in BH6 are: $OH + CH_4 \rightarrow CH_3 + H_2O$, $H + OH \rightarrow H_2 + O$, and $H + H_2S \rightarrow H_2 + HS$. Total energies at the left hand side, the right hand side, and the saddle point of these chemical reactions were evaluated, and the barrier heights of the forward (f) and reverse (r) reactions obtained by taking the relevant energy differences. We used the geometries provided in Ref. [103] and reference values from Ref. [98]. The results for various methods are summarized in Table VI.

DFA's such as LSDA, PBE, and SCAN underestimate barrier heights⁴⁵ by giving transition state energies that are too low compared to the reactant and product energies. An accurate description of the stretched bonds in the transition states requires full nonlocality in the exchange-correlation potential that the semi-local functionals cannot provide. Use of PZSIC reduces the overall errors, but in PZSIC-LSDA the barriers are still too small compared to reference values. This can be seen in the negative signed errors of all six barrier heights in Table VI. Applying LSIC-LSDA improves the barrier heights in almost every case. The MAE of the barrier heights improves from 17.6 kcal/mol for LSDA, to 4.9 in PZSIC-LSDA, to only 1.3 kcal/mol in LSIC-LSDA. Remarkably, as seen in the table, LSIC-LSDA has a smaller MAE than any of the methods listed, including PZSIC-PBE and PZSIC-SCAN.

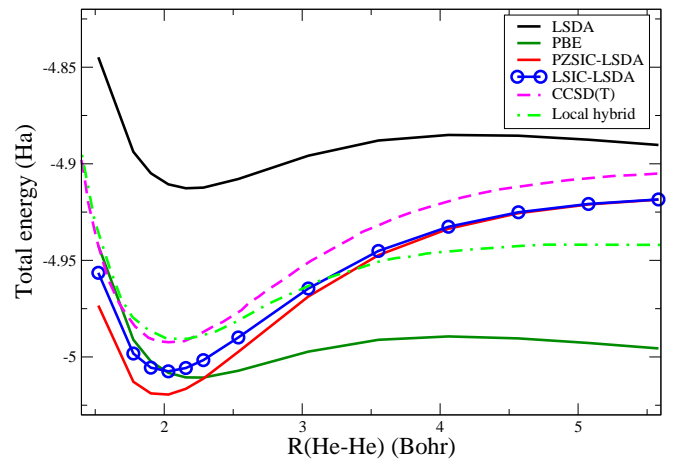
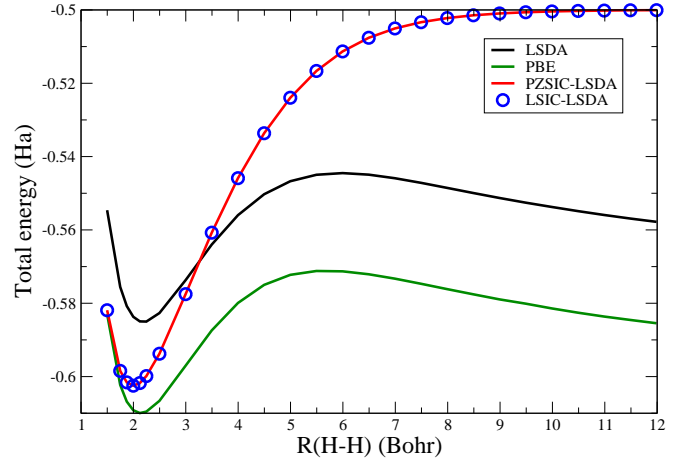


Figure 5. Ground-state dissociation curves for (a) H_2^+ and (b) He_2^+ . The CCSD(T)/cc-pVQZ results from Ref. [101] and local hybrid results from Ref. [102] are also shown for comparison.

IV. DISCUSSION

The LSIC method uses a point-wise scaling of SIC terms (Eqs. (8)–(10)) to reduce the effect of self-interaction in many-electron regions, while applying SIC at full strength in one-electron regions. We can think

Table V. SIE4×4 binding energy curves and SIE11 reaction energies (kcal/mol). Reference energies and signed errors are shown.

Reaction	R/R _e	Ref. ^a	PZSIC-LSDA ^b	LSIC-LSDA
$\text{H}_2^+ \rightarrow \text{H} + \text{H}^+$	1.0	64.4	0.0	0.0
	1.25	58.9	0.0	0.0
	1.5	48.7	0.0	0.0
	1.75	38.3	0.1	-0.1
$\text{He}_2^+ \rightarrow \text{He} + \text{He}^+$	1.0	56.9	5.8	-1.7
	1.25	46.9	1.9	-2.7
	1.5	31.3	-0.4	-3.0
	1.75	19.1	-1.6	-3.0
$(\text{NH}_3)_2^+ \rightarrow \text{NH}_3 + \text{NH}_3^+$	1.0	35.9	11.7	1.6
	1.25	25.9	7.3	6.7
	1.5	13.4	4.0	8.1
	1.75	4.9	3.4	6.7
$(\text{H}_2\text{O})_2^+ \rightarrow \text{H}_2\text{O} + \text{H}_2\text{O}^+$	1.0	39.7	5.8	0.4
	1.25	29.1	-1.4	4.2
	1.5	16.9	-2.7	1.5
	1.75	9.3	-1.5	1.8
$\text{C}_4\text{H}_{10}^+ \rightarrow \text{C}_2\text{H}_5 + \text{C}_2\text{H}_5^+$		35.28	11.44	-6.00
$(\text{CH}_3)_2\text{CO}^+ \rightarrow \text{CH}_3 + \text{CH}_3\text{CO}^+$		22.57	39.39	1.86
$\text{ClFCI} \rightarrow \text{ClCIF}$		-1.01	4.63	4.37
$\text{C}_2\text{H}_4 \dots \text{F}_2 \rightarrow \text{C}_2\text{H}_4 + \text{F}_2$		1.08	-0.23	-2.82
$\text{C}_6\text{H}_6 \dots \text{Li} \rightarrow \text{Li} + \text{C}_6\text{H}_6$		9.50	10.19	-13.50
$\text{NH}_3 \dots \text{ClF} \rightarrow \text{NH}_3 + \text{ClF}$		10.50	5.60	-4.56
$\text{NaOMg} \rightarrow \text{MgO} + \text{Na}$		69.56	28.56	11.45
$\text{FLiF} \rightarrow \text{Li} + \text{F}_2$		94.36	-4.82	-1.18
MAE SIE4×4			3.0	2.6
MAE SIE11 cationic			14.83	2.31
MAE SIE11 neutral			9.01	6.31

^a Reference¹⁰⁰.^b Reference⁷².

Table VI. BH6 forward (f) and reverse (r) barrier heights (kcal/mol). Signed errors are shown.

Reaction	Barrier	Ref. ^a	DFA			PZSIC			LSIC
			LSDA	PBE	SCAN	LSDA	PBE	SCAN	LSDA
$\text{OH} + \text{CH}_4 \rightarrow \text{CH}_3 + \text{H}_2\text{O}$	f	6.7	-23.6	-12.2	-8.3	-2.2	5.7	4.6	2.6
	r	19.6	-17.4	-10.7	-7.8	-12.5	-10.3	-7.1	-0.2
$\text{H} + \text{OH} \rightarrow \text{H}_2 + \text{O}$	f	10.7	-11.8	-2.2	-7.5	-1.1	2.3	0.0	-0.6
	r	13.1	-25.3	-9.9	-11.0	-4.8	2.9	1.8	1.2
$\text{H} + \text{H}_2\text{S} \rightarrow \text{H}_2 + \text{HS}$	f	3.6	-10.3	-4.8	-6.3	-1.7	1.7	-1.9	-1.3
	r	17.3	-17.2	-8.1	-6.2	-7.0	-2.1	-2.2	2.2
ME			-17.6	-8.0	-7.9	-4.9	0.0	-0.8	0.7
MAE			17.6	8.0	7.9	4.9	4.2	3.0	1.3

^a Reference⁹⁸.

of this as interior orbital scaling, in comparison with the exterior orbital scaling of Eq. (4). We showed in the previous section that using LSIC-LSDA results in significant performance gains for all the common electronic properties tested, as compared to both LSDA and PZSIC-LSDA. LSIC-LSDA improves on PZSIC for barrier heights and the SIE test sets where SIC is critical for getting physically reasonable results. For near-equilibrium properties where PZSIC degrades the performance of semilocal DFAs, LSIC-LSDA gives results that are better than PBE and nearly as good as SCAN. This

is remarkable, given the relative simplicity of LSDA compared to the semilocal functionals. It is worth comparing and contrasting LSIC-LSDA results with results using an exterior orbital scaling method, such as that presented in Ref. [45]. These authors suggest $k = 2$ as the best overall choice for use in Eq. (3) and (4). With this choice, the exterior orbital scaling method used with LSDA gives a MAE of 8.6 kcal/mol for the AE6 atomization energies. This is slightly better than the LSIC-LSDA result of 9.95 kcal/mol shown in Table IV. For the BH6 barrier heights, the global scaling method gives a MAE of 4.7

kcal/mol, compared to 1.3 kcal/mol for LSIC-LSDA (Table VI). While these results are similar, one should note that the global scaling approach causes the asymptotic form of the one electron potential to differ from the $-1/r$ form expected for the exact functional and maintained by PZSIC. This has an impact on properties that are sensitive to the nature of the potential in this region. For the HOMO eigenvalues of the atoms H–Kr, for example, our investigation shows that the MAE for PZSIC-LSDA is 0.672 eV, and that for the orbital-wise scaling approach of Eq. (3) and Eq. (4) is 1.034 eV ($k = 1$) when compared to the experimental IPs. Equality of the HOMO eigenvalue and the IP is a consequence of the linear variation of the total energy between adjacent integer numbers of electrons. This many-electron self-interaction freedom¹⁰¹ is exact for the exact functional and approximately true for PZSIC. It has been argued elsewhere¹⁰¹ that this property requires a full Hartree self-interaction correction term and thus should not be true for exterior orbital scaling corrections (or even for LSIC). A similar problem involves dissociating heteroatomic molecules to the correct neutral atom limits¹⁰¹. LSDA and the exterior orbital scaling method fail to do this in many cases, while PZSIC-LSDA succeeds. It is not yet clear how point-wise local scaling will affect such properties in general, since examining this requires fully self-consistent LSIC calculations. Preliminary *quasi* self-consistent LSIC calculations on the atomic systems using the weighted average of SIC potentials show that the self-consistency in fact slightly improves the LSIC results. The MAE in the HOMO eigenvalues of *quasi* self-consistent LSIC results is 0.363 eV, compared to the 0.672 eV of perturbative LSIC and 1.034 of exterior orbital scaling (cf. Eq. (4)). A full self-consistent implementation of LSIC-LSDA has been formulated and is being implemented into the FLOSIC code.

Recently, Santra and Perdew⁷⁸ showed that uniform electron gas norms satisfied by semi-local functionals are violated by the corresponding PZSIC-DFAs. To show how functionals behave in this limit, they fitted the calculated results for the exchange energy for neutral noble gas atoms using an exact large Z expansion of E_X as a fitting function. We used the same approach to test LSIC. We computed the LSIC-LSDA exchange energy of Ne, Ar, Kr, and Xe and then fitted these energies using the function,

$$\frac{E_X^{approx} - E_X^{exact}}{E_X^{exact}} \times 100\% = a + bx^2 + cx^3 \quad (14)$$

where $x = Z^{-1/3}$ and a , b , and c are fit parameters. The result is shown in Fig. 6. The value of a corresponds to the limit where $Z^{-1/3} \rightarrow 0$ which corresponds to the uniform density limit. a should vanish for the non-empirical LSDA, PBE, and SCAN functionals that are exact in this limit. The reported values of a are -0.18 , -0.06 , and -0.28 for LSDA, PBE, and SCAN and 5.79 , -3.30 , and -3.63 for PZSIC-LSDA, PZSIC-PBE, and PZSIC-SCAN⁷⁸. The small residual values of a for LSDA, PBE,

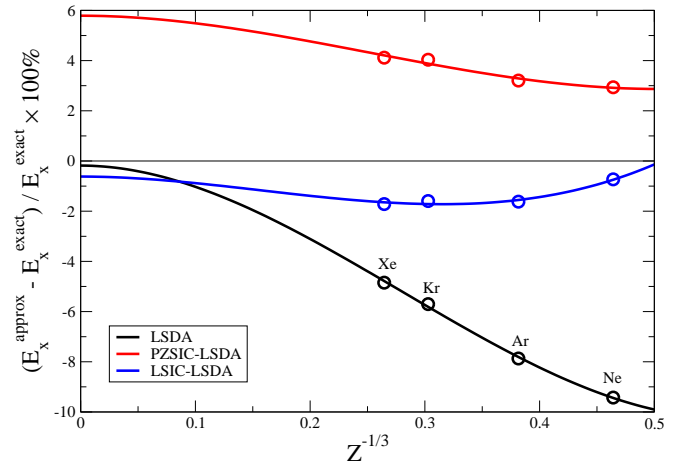


Figure 6. Percentage errors of the approximated exchange energies using the exact exchange energies as a reference. In LSIC-LSDA, $Z^{-1/3} \rightarrow 0$ limit is dramatically improved over PZSIC-LSDA.

and SCAN are due to errors in the extrapolations. For LSIC-LSDA, we obtain $a = -0.62$. We note that the scaling factor $z_\sigma(\vec{r}) = \tau_\sigma^W(\vec{r})/\tau_\sigma(\vec{r})$ we have chosen vanishes for a uniform density and that LSIC would therefore give no correction to LSDA in this limit. This may not be the case for a different choice of scaling factor. A constraint of the exact functional that is lost in PZSIC is thus recovered by LSIC (as by the exterior orbital scaling approach of Ref. [45]).

V. CONCLUSION

We introduced the LSIC-LSDA method that incorporates a point-wise scaling of self-interaction corrections based on a simple iso-orbital descriptor $z_\sigma = \tau_\sigma^W(\vec{r})/\tau_\sigma(\vec{r})$. The essential idea is to retain the benefit of PZSIC in the regions where the self-interaction is expected to be strong, while reducing its effect in other regions. We showed the results of LSIC-LSDA for a number of properties, including atomic total energies, IPs, and EAs for the atoms up to Kr, and atomization energies for a subset of G2 molecules and the AE6 molecules, dissociation and reaction energies of the SIE4×4 and SIE11 test sets, and chemical reaction barriers for the BH6 data set. In nearly all cases, the performance of LSIC is dramatically improved compared to both pure LSDA and PZSIC-LSDA. LSIC-LSDA even performs better than PBE for atomization energies and is competitive with SCAN in many cases, while keeping the benefits of PZSIC for properties like barrier heights, where the semi-local functions do poorly. We also showed that LSIC-LSDA restores the correct uniform density limit of the exchange energy that is lost in PZSIC. In all, LSIC-LSDA brings the full non-locality of the PZSIC method to bear for cases like stretched bonds where SIE effects are dominant, while maintaining the already good description of near equilib-

rium properties provided by semi-local functionals.

It is interesting to compare LSIC-LSDA with advancements made on the well-trodden path of creating and correcting more sophisticated semilocal functionals³¹. A major development along the latter was the introduction of a fraction of Hartree-Fock exchange which resulted in mitigating many deficiencies of the pure density functional approaches. As mentioned earlier, the formal justification for such mixing was the adiabatic connection between real interacting system and the non-interacting KS system. Because the exact exchange-correlation energy is an integral over coupling constant from 0 to 1, it could include some fraction of exact exchange, which is the correct integrand at the limit of zero coupling constant. It is interesting to see the parallels between this path and SIC. Because typical real systems are part-way between slowly-varying density and one-electron density limits, the exact exchange-correlation energy could include some fraction of PZSIC, which is exact for any one-electron density. The 50% scaling approach used by Jónsson and coworkers⁷⁵ can be considered as a global (orbital-independent) hybrid of DFA and PZSIC-DFA, in analogy to the traditional global hybrids. On the other hand, the present LSIC approach is analogous to local hybrids. Understanding obtained in the development of hybrid functionals may be beneficial in the further development of the LSIC method.

ACKNOWLEDGMENTS

The authors dedicate this paper to Dr. Mark Pederson on the occasion of his 60th birthday. R.R.Z. and Y.Y. acknowledge Drs. Luis Basurto and Jorge Vargas for discussions and technical assistance. This work was supported by the US Department of Energy, Office of Science, Office of Basic Energy Sciences, as part of the Computational Chemical Sciences Program under Award No. DE-SC0018331. The work of R.R.Z. was supported in part by the US Department of Energy, Office of Science, Office of Basic Energy Sciences, under Award No. DE-SC0006818. Support for computational time at the Texas Advanced Computing Center through NSF Grant No. TG-DMR090071, and at NERSC is gratefully acknowledged. R.R.Z. and Y.Y. conceived the LSIC concept and prepared the first draft of the manuscript. The other authors contributed calculations, figures, tables, references, discussions, and revision of the manuscript.

REFERENCES

- ¹W. Kohn and L. Sham, Phys. Rev. **140**, A1133 (1965).
- ²M. Levy, Proceedings of the National Academy of Sciences **76**, 6062 (1979).
- ³R. O. Jones and O. Gunnarsson, Rev. Mod. Phys. **61**, 689 (1989).
- ⁴R. O. Jones, Rev. Mod. Phys. **87**, 897 (2015).
- ⁵O. Gunnarsson and B. I. Lundqvist, Phys. Rev. B **13**, 4274 (1976).
- ⁶D. C. Langreth and J. P. Perdew, Solid State Commun. **17**, 1425 (1975).
- ⁷A. D. Becke, Phys. Rev. A **38**, 3098 (1988).
- ⁸J. P. Perdew, J. A. Chevary, S. H. Vosko, K. A. Jackson, M. R. Pederson, D. J. Singh, and C. Fiolhais, Phys. Rev. B **46**, 6671 (1992).
- ⁹J. P. Perdew, K. Burke, and Y. Wang, Phys. Rev. B **54**, 16533 (1996).
- ¹⁰J. P. Perdew, K. Burke, and M. Ernzerhof, Phys. Rev. Lett. **77**, 3865 (1996).
- ¹¹J. P. Perdew, S. Kurth, A. Zupan, and P. Blaha, Phys. Rev. Lett. **82**, 2544 (1999).
- ¹²J. P. Perdew and K. Schmidt, in *AIP Conference Proceedings*, Vol. 577 (AIP, 2001) pp. 1–20.
- ¹³H. Iikura, T. Tsuneda, T. Yanai, and K. Hirao, J. Chem. Phys. **115**, 3540 (2001).
- ¹⁴J. Tao, J. P. Perdew, V. N. Staroverov, and G. E. Scuseria, Phys. Rev. Lett. **91**, 146401 (2003).
- ¹⁵S. Lehtola, C. Steigemann, M. J. Oliveira, and M. A. Marques, SoftwareX **7**, 1 (2018).
- ¹⁶Y. Zhao and D. G. Truhlar, Acc. Chem. Res. **41**, 157 (2008).
- ¹⁷J. P. Perdew, A. Ruzsinszky, J. Tao, V. N. Staroverov, G. E. Scuseria, and G. I. Csonka, J. Chem. Phys. **123**, 062201 (2005), <https://doi.org/10.1063/1.1904565>.
- ¹⁸I. Lindgren, Int. J. Quantum Chem. **5**, 411 (1971).
- ¹⁹J. Perdew, Chem. Phys. Lett. **64**, 127 (1979).
- ²⁰M. S. Gopinathan, Phys. Rev. A **15**, 2135 (1977).
- ²¹A. Zunger, J. Perdew, and G. Oliver, Solid State Commun. **34**, 933 (1980).
- ²²O. Gunnarsson and R. O. Jones, Solid State Commun. **37**, 249 (1981).
- ²³A. D. Becke, J. Chem. Phys. **98**, 1372 (1993), <https://doi.org/10.1063/1.464304>.
- ²⁴D. Hait and M. Head-Gordon, J. Phys. Chem. Lett. **9**, 6280 (2018), <https://doi.org/10.1021/acs.jpclett.8b02417>.
- ²⁵J. Harris, Phys. Rev. A **29**, 1648 (1984).
- ²⁶J. Jaramillo, G. E. Scuseria, and M. Ernzerhof, J. Chem. Phys. **118**, 1068 (2003).
- ²⁷H. Iikura, T. Tsuneda, T. Yanai, and K. Hirao, J. Chem. Phys. **115**, 3540 (2001), <https://doi.org/10.1063/1.1383587>.
- ²⁸J. P. Perdew and A. Zunger, Phys. Rev. B **23**, 5048 (1981).
- ²⁹M. R. Pederson, R. A. Heaton, and C. C. Lin, J. Chem. Phys. **80**, 1972 (1984), <https://doi.org/10.1063/1.446959>.
- ³⁰M. R. Pederson, R. A. Heaton, and C. C. Lin, J. Chem. Phys. **82**, 2688 (1985), <https://doi.org/10.1063/1.448266>.
- ³¹M. R. Pederson and J. P. Perdew, Psi-k Newsletter **109**, 77 (2012).
- ³²J. Garza, J. A. Nichols, and D. A. Dixon, J. Chem. Phys. **112**, 7880 (2000), <https://doi.org/10.1063/1.481421>.
- ³³J. Garza, R. Vargas, J. A. Nichols, and D. A. Dixon, J. Chem. Phys. **114**, 639 (2001), <https://aip.scitation.org/doi/pdf/10.1063/1.1327269>.
- ³⁴S. Patchkovskii, J. Autschbach, and T. Ziegler, J. Chem. Phys. **115**, 26 (2001), <https://doi.org/10.1063/1.1370527>.
- ³⁵M. K. Harbola, Solid State Commun. **98**, 629 (1996).
- ³⁶S. Patchkovskii and T. Ziegler, J. Chem. Phys. **116**, 7806 (2002), <https://doi.org/10.1063/1.1468640>.
- ³⁷S. Patchkovskii and T. Ziegler, J. Phys. Chem. A **106**, 1088 (2002), <https://doi.org/10.1021/jp014184v>.

- ³⁸S. Goedecker and C. J. Umrigar, *Phys. Rev. A* **55**, 1765 (1997).
- ³⁹V. Polo, E. Kraka, and D. Cremer, *Mol. Phys.* **100**, 1771 (2002), <https://doi.org/10.1080/00268970110111788>.
- ⁴⁰V. Polo, J. Gräfenstein, E. Kraka, and D. Cremer, *Theor. Chim. Acta* **109**, 22 (2003).
- ⁴¹J. Gräfenstein, E. Kraka, and D. Cremer, *J. Chem. Phys.* **120**, 524 (2004), <https://doi.org/10.1063/1.1630017>.
- ⁴²J. Gräfenstein, E. Kraka, and D. Cremer, *Phys. Chem. Chem. Phys.* **6**, 1096 (2004).
- ⁴³O. A. Vydrov and G. E. Scuseria, *J. Chem. Phys.* **121**, 8187 (2004), <https://aip.scitation.org/doi/pdf/10.1063/1.1794633>.
- ⁴⁴O. A. Vydrov and G. E. Scuseria, *J. Chem. Phys.* **122**, 184107 (2005), <https://doi.org/10.1063/1.1897378>.
- ⁴⁵O. A. Vydrov, G. E. Scuseria, J. P. Perdew, A. Ruzsinszky, and G. I. Csonka, *J. Chem. Phys.* **124**, 094108 (2006), <https://doi.org/10.1063/1.2176608>.
- ⁴⁶R. R. Zope, M. K. Harbola, and R. K. Pathak, *The European Physical Journal D-Atomic, Molecular, Optical and Plasma Physics* **7**, 151 (1999).
- ⁴⁷O. A. Vydrov and G. E. Scuseria, *J. Chem. Phys.* **124**, 191101 (2006), <https://doi.org/10.1063/1.2204599>.
- ⁴⁸T. Tsuneda, M. Kamiya, and K. Hirao, *J. Chem. Phys.* **24**, 1592 (2003), <https://onlinelibrary.wiley.com/doi/pdf/10.1002/jcc.10279>.
- ⁴⁹J. B. Krieger, Y. Li, and G. J. Iafrate, *Phys. Rev. A* **45**, 101 (1992).
- ⁵⁰J. B. Krieger, Y. Li, and G. J. Iafrate, *Phys. Rev. A* **46**, 5453 (1992).
- ⁵¹U. Lundin and O. Eriksson, *Int. J. Quantum Chem.* **81**, 247 (2001).
- ⁵²Y. Li, J. B. Krieger, and G. J. Iafrate, *Phys. Rev. A* **47**, 165 (1993).
- ⁵³S. Lehtola, M. Head-Gordon, and H. Jónsson, *J. Chem. Theory Comput.* **12**, 3195 (2016).
- ⁵⁴G. I. Csonka and B. G. Johnson, *Theor. Chim. Acta* **99**, 158 (1998).
- ⁵⁵L. Petit, A. Svane, M. Lüders, Z. Szotek, G. Vaitheeswaran, V. Kanchana, and W. Temmerman, *J. Phys. Cond. Matter* **26**, 274213 (2014).
- ⁵⁶S. Kümmel and L. Kronik, *Rev. Mod. Phys.* **80**, 3 (2008).
- ⁵⁷T. Schmidt, E. Kraisler, L. Kronik, and S. Kümmel, *Phys. Chem. Chem. Phys.* **16**, 14357 (2014).
- ⁵⁸D.-y. Kao, M. Pederson, T. Hahn, T. Baruah, S. Liebing, and J. Kortus, *Magnetochemistry* **3**, 31 (2017).
- ⁵⁹S. Schwalbe, T. Hahn, S. Liebing, K. Treppe, and J. Kortus, *J. Comp. Chem.* **39**, 2463 (2018).
- ⁶⁰H. Jónsson, K. Tsemekhman, and E. J. Bylaska, in *Abstracts of Papers of the American Chemical Society*, Vol. 233 (American Chemical Society 1155 16TH ST, NW, Washington, DC 20036 USA, 2007) pp. 120–120.
- ⁶¹M. M. Rieger and P. Vogl, *Phys. Rev. B* **52**, 16567 (1995).
- ⁶²W. Temmerman, A. Svane, Z. Szotek, H. Winter, and S. Beiden, in *Electronic Structure and Physical Properties of Solids* (Springer, 1999) pp. 286–312.
- ⁶³M. Daene, M. Lueders, A. Ernst, D. Ködderitzsch, W. M. Temmerman, Z. Szotek, and W. Hergert, *J. Phys. Cond. Matter* **21**, 045604 (2009).
- ⁶⁴Z. Szotek, W. Temmerman, and H. Winter, *Physica B: Condensed Matter* **172**, 19 (1991).
- ⁶⁵J. Messud, P. M. Dinh, P.-G. Reinhard, and E. Suraud, *Phys. Rev. Lett.* **101**, 096404 (2008).
- ⁶⁶J. Messud, P. M. Dinh, P.-G. Reinhard, and E. Suraud, *Chem. Phys. Lett.* **461**, 316 (2008).
- ⁶⁷M. Lundberg and P. E. M. Siegbahn, *J. Chem. Phys.* **122**, 224103 (2005), <https://doi.org/10.1063/1.1926277>.
- ⁶⁸T. Körzdörfer, M. Mundt, and S. Kümmel, *Phys. Rev. Lett.* **100**, 133004 (2008).
- ⁶⁹T. Körzdörfer, S. Kümmel, and M. Mundt, *J. Chem. Phys.* **129**, 014110 (2008).
- ⁷⁰I. Ciofini, C. Adamo, and H. Chermette, *Chem. Phys.* **309**, 67 (2005).
- ⁷¹S. Lehtola and H. Jónsson, *J. Chem. Theory Comput.* **10**, 5324 (2014), pMID: 26583216, <https://doi.org/10.1021/ct500637x>.
- ⁷²Y. Yamamoto, C. M. Diaz, L. Basurto, K. A. Jackson, T. Baruah, and R. R. Zope, *The Journal of Chemical Physics* **151**, 154105 (2019), <https://doi.org/10.1063/1.5120532>.
- ⁷³E. Ö. Jónsson, S. Lehtola, and H. Jónsson, *Procedia Computer Science* **51**, 1858 (2015), international Conference On Computational Science, ICCS 2015.
- ⁷⁴J. P. Perdew, A. Ruzsinszky, J. Sun, and M. R. Pederson, in *Advances In Atomic, Molecular, and Optical Physics*, Vol. 64 (Academic Press, 2015) pp. 1 – 14.
- ⁷⁵S. Klüpfel, P. Klüpfel, and H. Jónsson, *J. Chem. Phys.* **137**, 124102 (2012).
- ⁷⁶S. Klüpfel, P. Klüpfel, and H. Jónsson, *Phys. Rev. A* **84**, 050501(R) (2011).
- ⁷⁷C. Shahi, P. Bhattarai, K. Wagle, B. Santra, S. Schwalbe, T. Hahn, J. Kortus, K. A. Jackson, J. E. Peralta, K. Treppe, S. Lehtola, N. K. Nepal, H. Myneni, B. Neupane, S. Adhikari, A. Ruzsinszky, Y. Yamamoto, T. Baruah, R. R. Zope, and J. P. Perdew, *J. Chem. Phys.* **150**, 174102 (2019).
- ⁷⁸B. Santra and J. P. Perdew, *J. Chem. Phys.* **150**, 174106 (2019), <https://doi.org/10.1063/1.5090534>.
- ⁷⁹R. R. Zope, T. Baruah, Y. Yamamoto, L. Basurto, C. Diaz, J. Peralta, K. A. Jackson, and V. J., FLOSIC 0.1.2, based on the NRLMOL code of M. R. Pederson.
- ⁸⁰Y. Yamamoto, L. Basurto, C. M. Diaz, R. R. Zope, and T. Baruah, Self-interaction correction to density functional approximations using Fermi-Löwdin orbitals: Methodology and Parallelization, based on UTEP-NRLMOL code.
- ⁸¹M. R. Pederson, A. Ruzsinszky, and J. P. Perdew, *J. Chem. Phys.* **140**, 121103 (2014), <https://doi.org/10.1063/1.4869581>.
- ⁸²M. R. Pederson and T. Baruah, in *Advances In Atomic, Molecular, and Optical Physics*, Vol. 64 (Academic Press, 2015) pp. 153 – 180.
- ⁸³K. P. K. Withanage, S. Akter, C. Shahi, R. P. Joshi, C. Diaz, Y. Yamamoto, R. Zope, T. Baruah, J. P. Perdew, J. E. Peralta, and K. A. Jackson, *Phys. Rev. A* **100**, 012505 (2019).
- ⁸⁴A. Johnson, K. P. K. Withanage, K. Sharkas, Y. Yamamoto, T. Baruah, R. Zope, J. E. Peralta, and K. A. Jackson, unpublished.
- ⁸⁵K. Sharkas, L. Li, K. Treppe, K. P. K. Withanage, R. P. Joshi, R. R. Zope, T. Baruah, J. K. Johnson, K. A. Jackson, and J. E. Peralta, *J. Phys. Chem. A* **122**, 9307 (2018), pMID: 30412407.
- ⁸⁶M. Pederson, D. Porezag, J. Kortus, and D. Patton, *Physica Status Solidi (b)* **217**, 197 (2000).
- ⁸⁷M. R. Pederson and K. A. Jackson, *Phys. Rev. B* **41**, 7453 (1990).
- ⁸⁸K. A. Jackson and M. R. Pederson, *Phys. Rev. B* **42**, 3276 (1990).
- ⁸⁹D. Porezag and M. R. Pederson, *Phys. Rev. A* **60**, 2840 (1999).
- ⁹⁰S. Schwalbe, T. Hahn, S. Liebing, K. Treppe, and J. Kortus, *J. Comp. Chem.* **39**, 2463 (2018), <https://onlinelibrary.wiley.com/doi/pdf/10.1002/jcc.25586>.
- ⁹¹M. R. Pederson, *J. Chem. Phys.* **142**, 064112 (2015), <https://doi.org/10.1063/1.4907592>.
- ⁹²Z.-h. Yang, M. R. Pederson, and J. P. Perdew, *Phys. Rev. A* **95**, 052505 (2017).
- ⁹³D.-y. Kao, K. Withanage, T. Hahn, J. Batool, J. Kortus, and K. Jackson, *J. Chem. Phys.* **147**, 164107 (2017),

- <https://doi.org/10.1063/1.4996498>.
- ⁹⁴R. P. Joshi, K. Trepte, K. P. K. Withanage, K. Sharkas, Y. Yamamoto, L. Basurto, R. R. Zope, T. Baruah, K. A. Jackson, and J. E. Peralta, *J. Chem. Phys.* **149**, 164101 (2018).
- ⁹⁵S. J. Chakravorty, S. R. Gwaltney, E. R. Davidson, F. A. Parpia, and C. F. Fischer, *Phys. Rev. A* **47**, 3649 (1993).
- ⁹⁶National Institute of Standards and Technology, NIST Computational Chemistry Comparison and Benchmark Database NIST Standard Reference Database Number 101 Release 19, April 2018, Editor: Russell D. Johnson III <http://cccbdb.nist.gov/> DOI:10.18434/T47C7Z.
- ⁹⁷L. A. Curtiss, K. Raghavachari, G. W. Trucks, and J. A. Pople, *J. Chem. Phys.* **94**, 7221 (1991), <https://doi.org/10.1063/1.460205>.
- ⁹⁸B. J. Lynch and D. G. Truhlar, *J. Phys. Chem. A* **107**, 8996 (2003), <https://doi.org/10.1021/jp035287b>.
- ⁹⁹L. Goerigk, A. Hansen, C. Bauer, S. Ehrlich, A. Najibi, and S. Grimme, *Phys. Chem. Chem. Phys.* **19**, 32184 (2017).
- ¹⁰⁰L. Goerigk and S. Grimme, *J. Chem. Theory Comput.* **6**, 107 (2010), pMID: 26614324, <https://doi.org/10.1021/ct900489g>.
- ¹⁰¹A. Ruzsinszky, J. P. Perdew, G. I. Csonka, O. A. Vydrov, and G. E. Scuseria, *J. Chem. Phys.* **126**, 104102 (2007), <https://doi.org/10.1063/1.2566637>.
- ¹⁰²T. Schmidt, E. Kraisler, A. Makkamal, L. Kronik, and S. Kummel, *The Journal of Chemical Physics* **140**, 18A510 (2014), <https://doi.org/10.1063/1.4865942>.
- ¹⁰³J. Zheng, Y. Zhao, and D. G. Truhlar, *J. Chem. Theory Comput.* **3**, 569 (2007), pMID: 26637036, <https://doi.org/10.1021/ct600281g>.